

Addendum VFPS proposal : Acceptances

L. Favart, D. Johnson, P. Marage, R. Roosen,

Inter-University Institute for High Energies ULB-VUB, Brussels, Belgium

E.A. De Wolf, P. Van Mechelen, T. Anthonis

Universitaire Instelling Antwerpen, Wilrijk, Belgium

L. Jönsson, H. Jung,

Physics Department, University of Lund, Lund, Sweden

V. Blobel, F. Büsser, V. Jemanov, A. Meyer, B. Naroska, F. Niebergall, J. Schütt, H. Spitzer, R. vanStaa

University Hamburg II Institut f. Experimentalphysik, Hamburg, Germany

P.R. Newman,

School of Physics and Space Research, University of Birmingham, Birmingham, UK

1 Process acceptances

The present note is a supplement to the VFPS proposal H1-5/00-582 (PRC 01/00), in which the VFPS acceptance regarding the different processes presented in the proposal are further detailed. Attention will be given to the hard processes of jet and charm production. Also vector meson production at high Q^2 and deep virtual compton scattering process (DVCS) will be discussed. Acceptances will be given as a function of the pertinent variables Q^2, W, x_P, \dots

In the proposal the nominal VFPS position w.r.t. the proton beam is the “12 σ location”. To avoid a possible background of coasting beam, the VFPS could be positioned an extra 3 mm away from the proton beam line. The effect on the acceptance for the different processes will be labelled in the following figures as “VFPS-shifted” or “VFPS+3 ”mm.

Finally to indicate “ a figure of merit” of the VFPS w.r.t the existing proton spectrometers we also show the acceptance for the various processes for the FPS - 80 meter pot (horizontal).

In summary, the following curves will be shown on the distributions

1. no VFPS tagging (H1-acceptance)

2. VFPS tagging, with VFPS at the 12σ location
3. VFPS tagging, with VFPS at the $12\sigma + 3\text{ mm}$ location
4. FPS tagging by 80 m pot

For items 2-4, full event containment in H1 is assumed.

2 Charm and Jets

In order to determine the various acceptance regions for jets, the following (standard) selection criteria have been applied

$$0.1 < y < 0.7, \quad 4 < Q^2 < 80 \text{ GeV}^2 \quad x_{\mathbb{P}} < 0.05 \quad \text{and} \quad p_t^{\text{Jets}} > 4 \text{ GeV in } \gamma^*p \text{ CMS}$$

Fig. 1 shows the accepted jet events as a function of $x_{\mathbb{P}}$, p_t , Q^2 and M_X for the different conditions (1-4). The acceptance for jet events in the VFPS relative to the H1 acceptance amounts to 70%, mainly

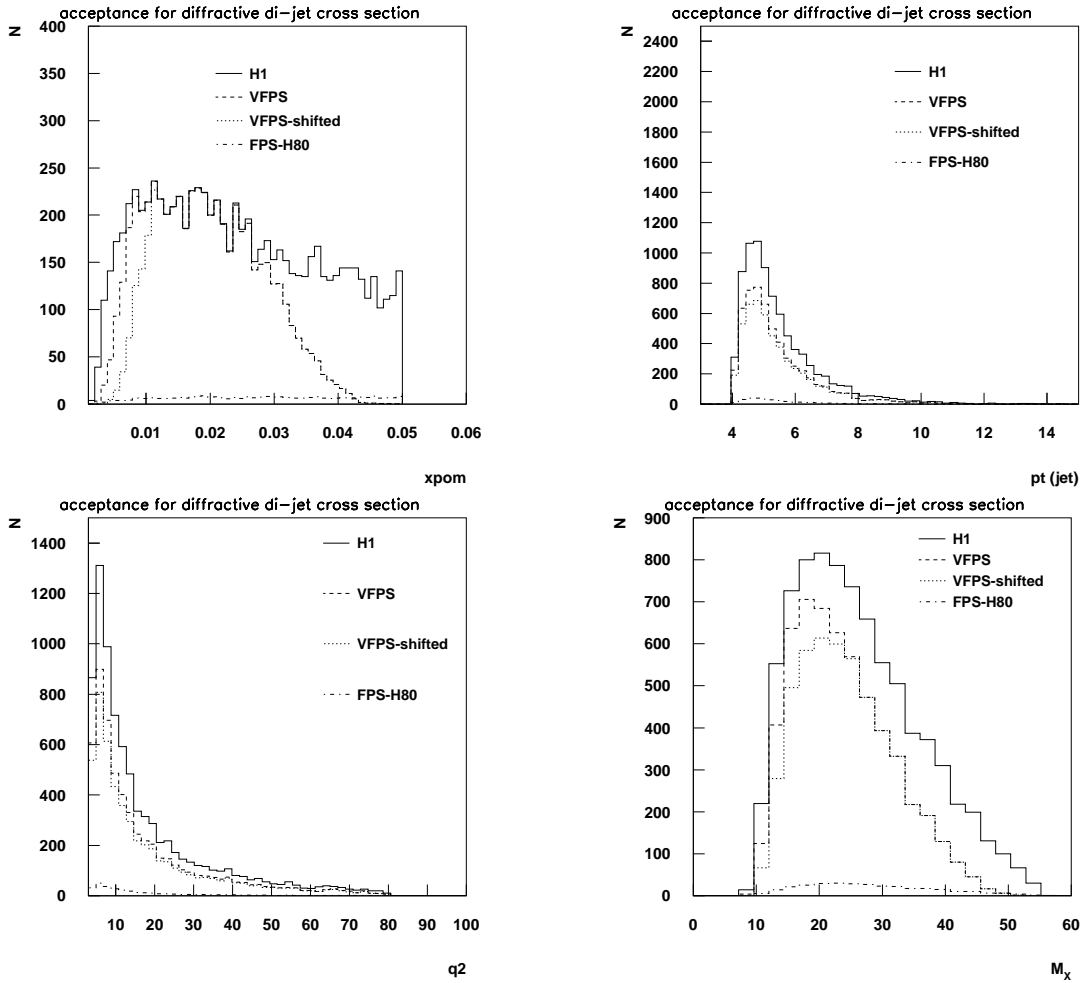


Figure 1: Jet events observed in H1 (full), VFPS tagged at 12σ (dashed), VFPS tagged at $12\sigma+3\text{mm}$ (dotted) and FPS tagged (dash-dotted) as a function of $x_{\mathbb{P}}$, p_t , Q^2 and M_X .

determined by the VFPS acceptance at large $x_{\mathbb{P}}$. For an upper limit in $x_{\mathbb{P}} < 0.03$ this percentage increases to 91 %. However in the small $x_{\mathbb{P}}$ region, the truly diffractive region, the difference in acceptance between H1, the VFPS and the shifted VFPS position is rather small. This is not unexpected as the large required jet energy is setting the lower bound on $x_{\mathbb{P}}$. The very limited acceptance in all variables of the FPS 80 meter pot is also indicated.

For charm, the following D^* selection criteria are used

$$0.05 < y < 0.7, \quad 2 < Q^2 < 100 \text{ GeV}^2 \quad x_{\mathbb{P}} < 0.04$$

$$; \text{ in lab } \quad p_t^{D^*} > 2 \text{ GeV} \quad \text{and} \quad |\eta| < 1.5$$

Fig. 2 shows the accepted charm events as a function of Q^2 , p_t and $x_{\mathbb{P}}$ in the 4 different situations. The conclusions are similar to those of the jet sample. The lower charm mass in comparison with the jet energy increases the acceptance difference in the various situations at low $x_{\mathbb{P}}$. The relative acceptance with respect to H1 is 70 % which amounts to approximately 450 events. If, as for the jets we assume an $x_{\mathbb{P}} < 0.03$ upper limit, the relative acceptance increases to 77 %. Being interested in the large Q^2 events after the lumi upgrade, an additional $Q^2 > 10 \text{ GeV}^2$ cut further increases the number to 84%.

In summary, for the processes with a hard scale the fraction of accepted events in the $x_{\mathbb{P}}$ range $[5 \cdot 10^{-3}, 3 \cdot 10^{-2}]$ exceeds the 80%.

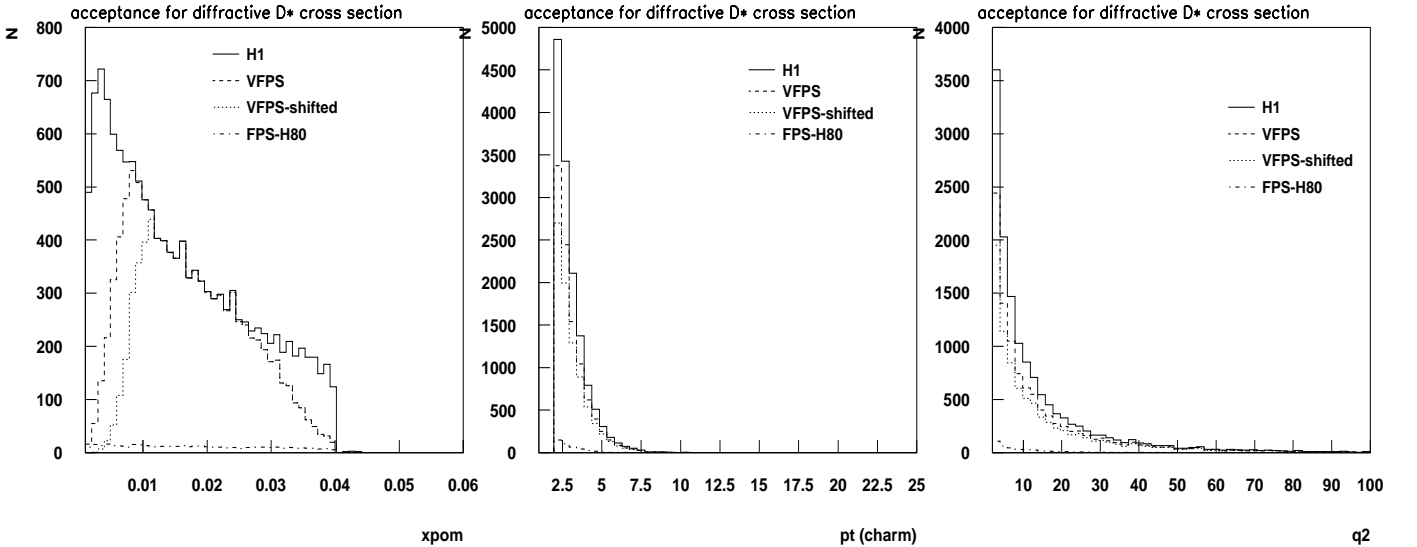


Figure 2: Charm events observed in H1 (full), VFPS tagged at 12σ (dashed), VFPS tagged at $12\sigma+3\text{mm}$ (dotted) and FPS tagged (dash-dotted) as a function of $x_{\mathbb{P}}$, p_t , Q^2 .

3 Vector mesons ρ and J/Ψ

In the acceptance calculation for vector mesons, we have assumed that up to a scale of $Q^2 \approx 20 \text{ GeV}^2$, the physics will be covered by the data accumulated up to the shutdown. Therefore in fig. 3 and fig. 4, the Q^2 , W and $x_{\mathbb{P}}$ distributions for the accepted ρ (J/Ψ) events are shown for $Q^2 > 20 \text{ GeV}^2$. In contrast to the jet and charm events, where the acceptance limitations from the VFPS are small, in the case of vector mesons, the VFPS imposed $x_{\mathbb{P}}$ range constrains the W acceptance to lower W values (see fig 3).

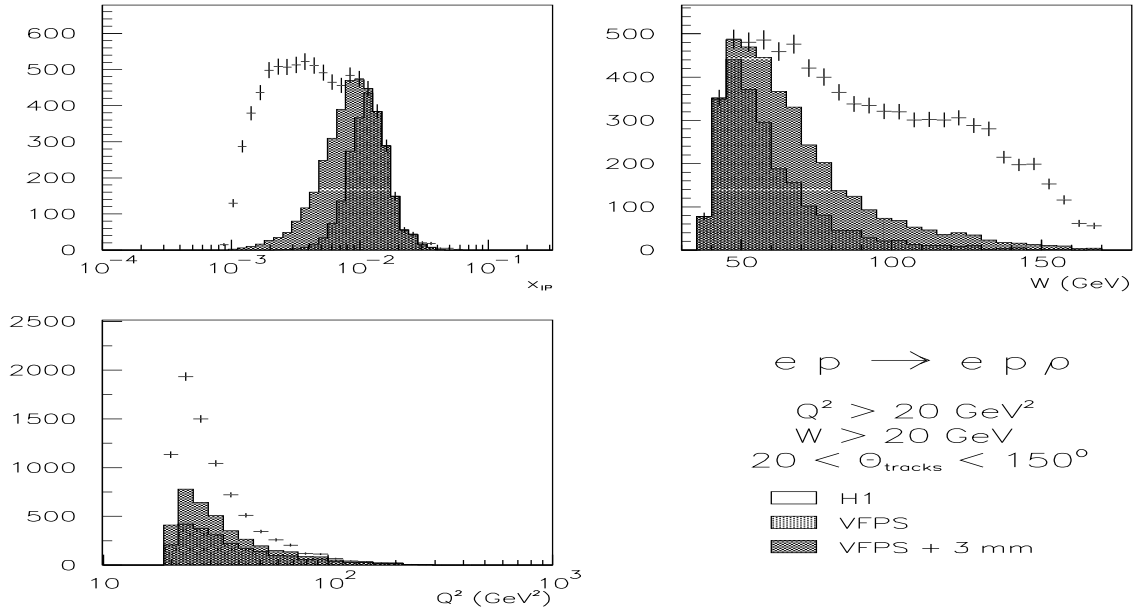


Figure 3: $e + p \rightarrow e + \rho + p$: events observed in H1 (full), VFPS tagged at 12σ (light) and VFPS tagged at $12\sigma+3\text{mm}$ (dark) as a function of Q^2 , W and x_{IP} .

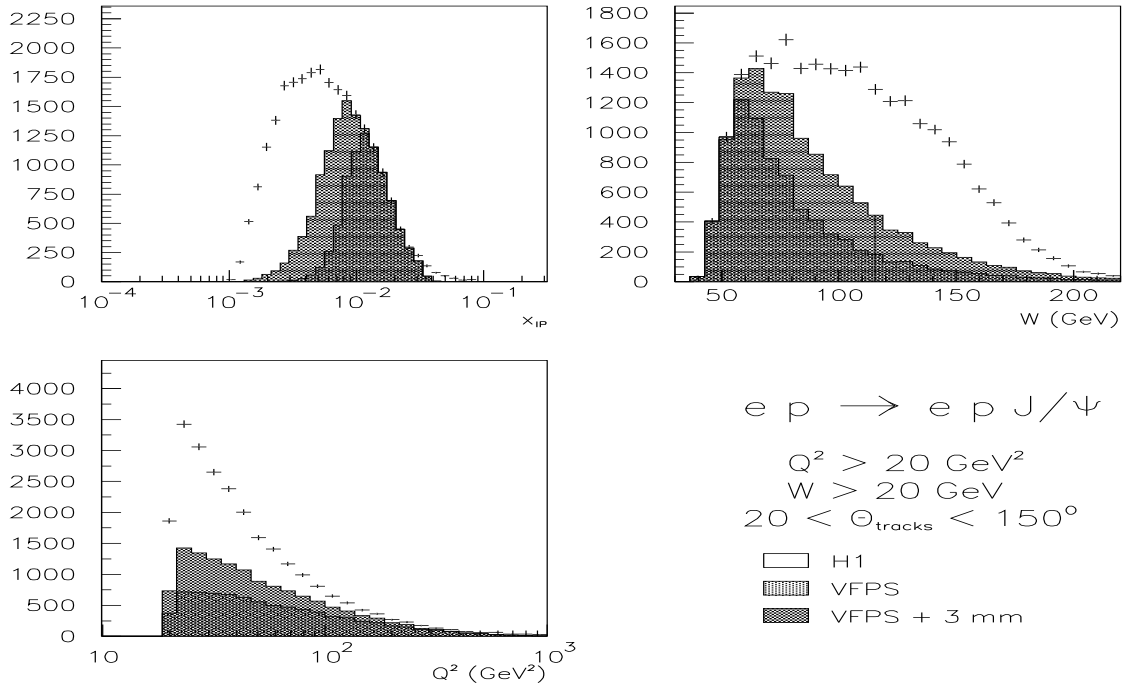


Figure 4: $e + p \rightarrow e + J/\Psi + p$: events observed in H1 (full), VFPS tagged at 12σ (light) and VFPS tagged at $12\sigma+3\text{mm}$ (dark) as a function of x_{IP} , W and Q^2 .

For the J/Ψ , although the W-acceptance is somewhat larger, conclusions similar to the ρ sample hold (see fig 4).

The acceptance differences between the VFPS and FPS for vector meson production are show in table 1 for two cuts in Q^2 .

$e + p \rightarrow e + p + \rho, J/\Psi \quad W > 20 \text{ GeV}$				
Process	Accep. VFPS (%) $Q^2 > 10 \text{ GeV}^2$	Accep. VFPS (%) $Q^2 > 20 \text{ GeV}^2$	Accep. FPS (%) $Q^2 > 10 \text{ GeV}^2$	Accep. FPS $Q^2 > 20 \text{ GeV}^2$
$ep \rightarrow ep\rho$	32	47	2.3	2.4
$ep \rightarrow epJ/\Psi$	43	53	2.4	2.5

Table 1: VFPS and FPS acceptance for ρ and J/Ψ production.

4 DVCS process

As for the ρ sample, we have assumed again that up to a scale of $Q^2 \approx 20 \text{ GeV}^2$, the physics will be covered by the data accumulated up to the shutdown. Fig. 5 shows the acceptance for the reaction

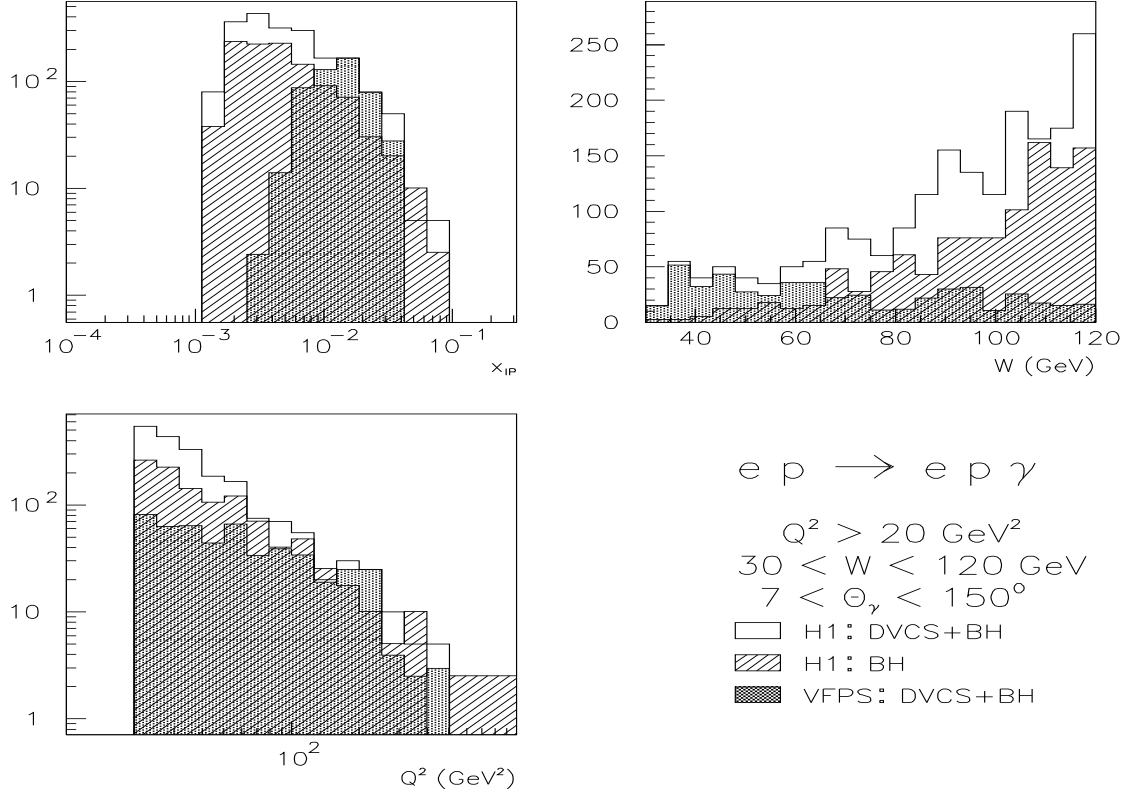


Figure 5: $ep \rightarrow ep\gamma$: events observed in H1 (full), VFPS tagged at 12σ (dark), Bethe Heitler contribution (hatched) as a function of a) x_{IP} , b) W and c) Q^2 .

$ep \rightarrow ep\gamma$, including the DVCS and Bethe Heitler processes, as a function of x_p , W and Q^2 . At low W where the DVCS process dominates, most of the events will be tagged. The lower cutoff on W is imposed by the H1 detector acceptance not by the VFPS. Table 2 shows the relative acceptance for $ep \rightarrow ep\gamma$ events in H1, VFPS and FPS.

$e + p \rightarrow e + p + \gamma \quad 30 < W < 120 \text{ GeV}$			
	Acc(H1)(events)	Acc(VFPS)(%)	Acc(FPS)(%)
$Q^2 > 20 \text{ GeV}^2$	1950	26	2.5

Table 2: Acceptance for the reaction $ep \rightarrow ep\gamma$ for H1, VFPS and FPS.